

III-V Nitride Light-Emitting Diodes

Shuji Nakamura

*Department of Research and Development, Nichia Chemical Industries, Ltd., 491 Oka,
Kaminaka, Anan, Tokushima 774, Japan*

Abstract

Highly efficient InGaN/AlGaIn double-heterostructure blue-light-emitting diodes (LEDs) with an external quantum efficiency of 5.4 % were fabricated by codoping Zn and Si into an InGaIn active layer. The output power was as high as 3 mW at a forward current of 20 mA. The peak wavelength and the full width at half-maximum of the electroluminescence of blue LEDs were 450 nm and 70 nm, respectively. Blue-green LEDs with a brightness of 2 cd and a peak wavelength of 500 nm were fabricated for application to traffic lights, by increasing the indium mole fraction of the InGaIn active layer.

Introduction

Much research has been done on high-brightness blue LEDs and LDs for use in full-color displays, full-color indicators and light sources for lamps with the characteristics of high efficiency, high reliability and high speed. For these purposes, II-VI materials such as ZnSe[1], SiC[2] and III-V nitride semiconductors such as GaN[3] have been investigated intensively for a long time. However, it has been impossible to obtain high-brightness blue LEDs with brightness over 1 cd and LDs. Recent research on III-V nitrides has paved the way for realization of high-quality crystals of AlGaIn and InGaIn, and p-type conduction in AlGaIn [4-12]. Also, the hole-compensation mechanism of p-type AlGaIn has been elucidated [13-17]. High-brightness blue and blue-green LEDs with a luminous intensity of 1 cd have been achieved by using these techniques and are now commercially available [4,5]. Here, the present status and performance of III-V nitride visible light emitting devices are described.

Experimental

InGaIn/AlGaIn structure was grown by the two-flow metalorganic chemical vapor deposition (MOCVD) method. Details of the two-flow MOCVD are described

in other papers [18,19]. The growth was conducted at atmospheric pressure. Sapphire with (0001) orientation (C face) and two inches in diameter, was used as a substrate. Trimethylgallium (TMG), trimethylaluminum (TMA), trimethylindium (TMI), monosilane (SiH_4), bis-cyclopentadienyl magnesium (Cp_2Mg), diethylzinc (DEZ) and ammonia (NH_3) were used as Ga, Al, In, Si, Mg, Zn and N sources, respectively. For InGaIn growth, triethylgallium (TEG) was used as the Ga source. First, the substrate was heated to 1050 °C in a stream of hydrogen. Then, the substrate temperature was lowered to 510 °C for growth of the GaIn buffer layer. The thickness of the GaIn buffer layer was about 300 Å. Next, the substrate temperature was elevated to 1020 °C for growth of GaIn films. During the deposition, the flow rates of NH_3 , TMG and SiH_4 (10 ppm SiH_4 in H_2) in the main flow were maintained at 4.0 l/min, 30 $\mu\text{mol/min}$ and 4 nmol/min, respectively. The flow rates of H_2 and N_2 in the subflow were both maintained at 10 l/min. The Si-doped GaIn films were grown for 60 minutes. The thickness of Si-doped GaIn film was approximately 4 μm . After GaIn growth, a Si-doped $\text{Al}_{0.15}\text{Ga}_{0.85}\text{N}$ layer was grown to the thickness of 0.15 μm by flowing TMA and TMG. After $\text{Al}_{0.15}\text{Ga}_{0.85}\text{N}$ growth, the temperature was decreased to 800 °C, and the Zn- and Si-codoped $\text{In}_{0.06}\text{Ga}_{0.94}\text{N}$ layer was grown for 20 minutes. During the $\text{In}_{0.06}\text{Ga}_{0.94}\text{N}$ deposition, the flow rates of TMI, TEG and NH_3 in the main flow were maintained at 17 $\mu\text{m/min}$, 1.0 $\mu\text{mol/min}$ and 4.0 l/min, respectively. Zn and Si were codoped into InGaIn films by introducing DEZ and SiH_4 during InGaIn growth at the flow rates of 10 nmol/min and 1 nmol/min, respectively. The thickness of the InGaIn layer was about 1000 Å. After the InGaIn growth, the temperature was increased to 1020 °C for growth of Mg-doped p-type $\text{Al}_{0.15}\text{Ga}_{0.85}\text{N}$ and GaIn

layers by flowing TMA, TMG and Cp_2Mg gases. The thicknesses of Mg-doped p-type $\text{Al}_{0.15}\text{Ga}_{0.85}\text{N}$ and GaN layers were 0.15 μm and 0.5 μm , respectively. A p-type GaN layer was used as a contact layer for a p-type electrode in order to improve the ohmic contact. After the growth, N_2 ambient thermal annealing was performed to obtain a highly p-type GaN layer at a temperature of 700 $^\circ\text{C}$. Fabrication of LED chips was accomplished as follows: the surface of the p-type GaN layer was partially etched until the n-type GaN layer was exposed. Next, a Ni/Au contact was evaporated onto the p-type GaN layer and Ti/Al contact onto the n-type GaN layer. The wafer was cut into a rectangular shape. These chips were set on the lead frame, and were then molded. The characteristics of LEDs were measured under DC-biased conditions at room temperature. Figure 1 shows the structure of the InGaN/AlGaIn DH LEDs.

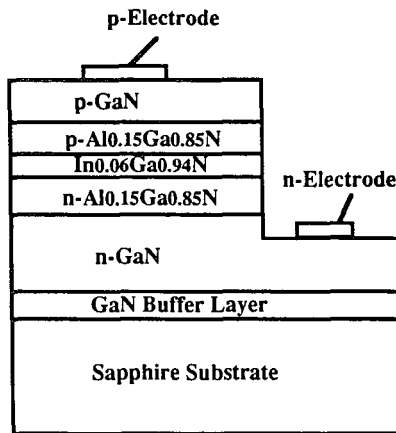


Figure 1. The structure of the InGaN/AlGaIn DH LEDs.

Results and Discussions

Figure 2 shows the band-gap energy of grown InGaN films as a function of the indium mole fraction X . The band-gap energy was obtained by room-temperature PL measurements assuming that the narrow sharp emissions in the violet and blue regions are BE emissions. The indium mole fraction of the InGaN films was determined by the measurements of X-ray diffraction peaks. Osamura et al. [20] have already shown that E_g in ternary alloys $\text{In}_X\text{Ga}_{(1-X)}\text{N}$ obeys a parabolic relationship with the molar fraction X :

$$E_g(X) = XE_{g,\text{InN}} + (1-X)E_{g,\text{GaN}} - bX(1-X), \quad (1)$$

where $E_g(X)$ represents the band-gap energy of $\text{In}_X\text{Ga}_{(1-X)}\text{N}$, $E_{g,\text{InN}}$ and $E_{g,\text{GaN}}$ represent the band-gap energy of compounds InN and GaN, respectively,

and b is the bowing parameter [20]. In that calculation, $E_{g,\text{InN}}$ was 1.95 eV, $E_{g,\text{GaN}}$ was 3.40 eV and b was 1.00 eV. These values calculated using eq. (1) are shown by the solid curve in Fig. 2. Although our experimental values, which were obtained by PL and X-ray diffraction measurements on single-crystal InGaN films, fluctuate slightly, the solid curve fits our experimental data quite well between indium mole fractions $X=0.07$ and $X=0.33$. Therefore, it is concluded that Osamura et al.'s [20] results can be used to estimate the relationship between band-gap energy and indium mole fraction X in our study quite well, assuming that the band-gap energies for GaN and InN are 3.40 and 1.95 eV, respectively.

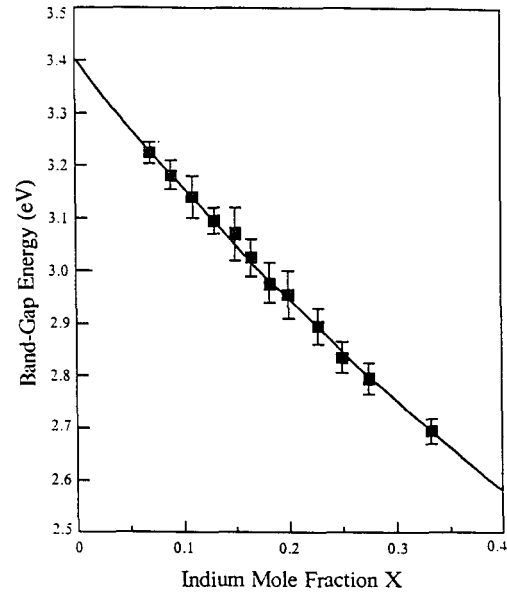


Figure 2. Band-gap energy of $\text{In}_X\text{Ga}_{(1-X)}\text{N}$ films as a function of the indium mole fraction X . The indium mole fraction X was determined by measurements of the X-ray diffraction peaks. Solid curve represents values which were obtained by eq. (1) as discussed in the text, assuming that the band-gap energies for GaN and InN are 3.40 and 1.95 eV, respectively.

Next, Si and Zn were codoped into the above-mentioned InGaN films in order to obtain longer-wavelength blue emission centers which have a luminous intensity high enough to be detected by human eyes. The luminous intensity of the violet emission originating from $\text{In}_X\text{Ga}_{(1-X)}\text{N}$ ($X < 0.2$) band-to-band recombination is insufficient for practical use in visible LEDs. Figure 3 shows a typical room-temperature PL of Si- and Zn-codoped InGaN film grown on GaN film. During InGaN growth, SiH_4 and DEZ were introduced at the same time to codope both Si and Zn into InGaN. Broad strong emission is observed around 460 nm, which is considered to originate from impurity-assisted recombination in Si-

and Zn-codoped InGa_N film. In the shorter-wavelength region, a weak peak can be observed around 385 nm, which is considered to be BE emission of InGa_N. Zn doping into InGa_N show values between 0.4 eV and 0.5 eV lower than the BE emission energy of InGa_N as a Zn-related emission energy. The indium mole fraction was determined by calculating the peak difference between Ga_N and InGa_N peaks in the double-crystal XRC measurement. The calculated value of the indium mole fraction of this sample was 0.06.

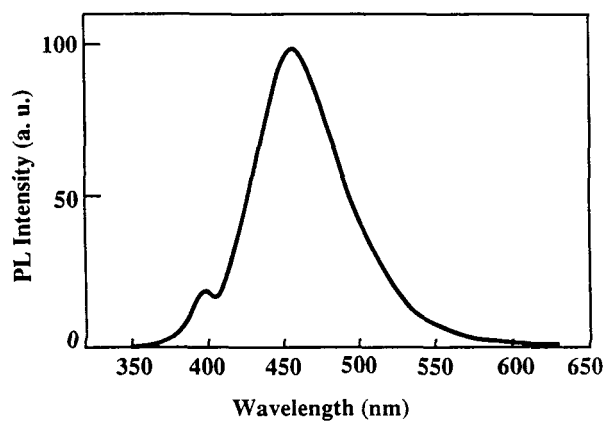


Figure 3. Typical room-temperature PL of Si- and Zn-codoped In_{0.06}Ga_{0.94}N film grown on GaN film.

Figure 4 shows the electroluminescence (EL) spectra of the InGa_N/AlGa_N DH LEDs at forward currents of 0.1 mA, 1 mA and 20 mA. The carrier concentration of the InGa_N active layer in this LED was $1 \times 10^{19} \text{ cm}^{-3}$. A typical peak wavelength and full width at half-maximum (FWHM) of the EL were 450 nm and 70 nm, respectively, at 20 mA. The peak wavelength shifts to shorter wavelengths with increasing forward current. The peak wavelength is 460 nm at 0.1 mA, 449 nm at 1 mA and 447 nm at 20 mA. This blue shift of EL spectra with increasing forward current suggests that the luminescence mechanism is the DA pair recombination in the InGa_N active layer codoped with both Si and Zn. At 20 mA, a narrower, higher-energy peak emerges around 385 nm, as shown in Fig. 4. This peak is due to band-to-band recombination in the InGa_N active layer. This peak becomes resolved at injection levels where the impurity-related recombination is saturated. The output power of the InGa_N/AlGa_N DH blue LEDs is 1.5 mW at 10 mA, 3 mW at 20 mA and 4.8 mW at 40 mA. The external quantum efficiency is 5.4 % at 20 mA. The typical on-axis luminous intensity of InGa_N/AlGa_N LEDs with 15° conical viewing angle is

2.5 cd at 20 mA. This luminous intensity is the highest value ever reported for blue LEDs. The forward voltage was 3.6 V at 20 mA.

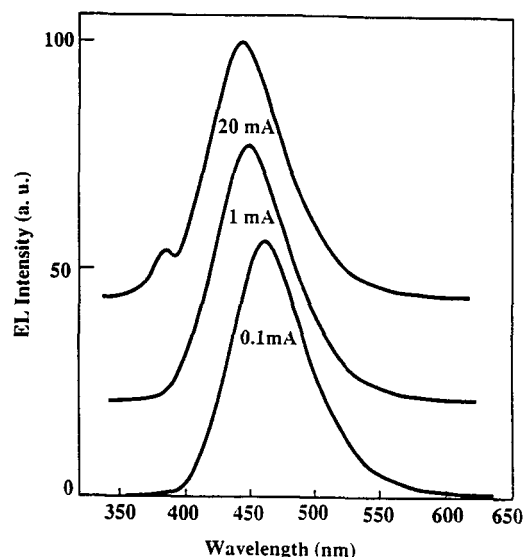


Figure 4. EL spectra of the InGa_N/AlGa_N DH blue LEDs under different forward currents.

Blue-green LEDs were fabricated for application to traffic lights by increasing the indium mole fraction of the InGa_N active layer from 0.06 to 0.19 in the blue LEDs. Figure 5 shows the EL spectra of the blue-green InGa_N/AlGa_N DH LEDs at forward currents of 0.5 mA, 1 mA and 20 mA. A typical peak wavelength and a FWHM of the EL were 500 nm and 80 nm, respectively, at 20 mA. The peak wavelength shifts to shorter wavelengths with increasing forward current. The peak wavelength is 537 nm at 0.5 mA, 525 nm at 1 mA and 500 nm at 20 mA. This blue shift of EL spectra with increasing forward current also suggests that the luminescence mechanism is DA pair recombination in the InGa_N active layer codoped with both Si and Zn. The output power of the InGa_N/AlGa_N DH blue-green LEDs is 1.2 mW at 20 mA. The external quantum efficiency is 2.4 % at 20 mA. A typical on-axis luminous intensity of InGa_N/AlGa_N blue-green LEDs with 15° conical viewing angle is 2 cd at 20 mA. This luminous intensity is the highest value ever reported for blue-green LEDs. Also, this luminous intensity is sufficiently bright for outdoor application, such as traffic lights and displays. The forward voltage was 3.5 V at 20 mA.

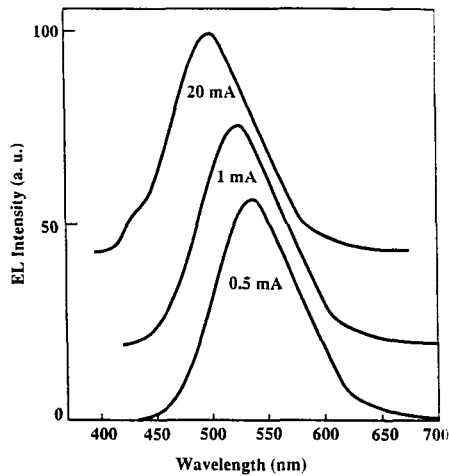


Figure 5. EL spectra of the InGaN/AlGaIn DH blue-green LEDs under different forward currents.

Figure 6 shows the EL spectrum of the InGaN/AlGaIn DH violet LEDs at forward current of 10 and 20 mA. These violet LEDs were grown under the same conditions as blue and blue-green LEDs, except for the InGaN active layer. During InGaN growth, only Si was doped without Zn. The typical output power was 1.5 mW and the external quantum efficiency was as high as 2.3 % at a forward current of 20 mA at room temperature. The peak wavelength and the FWHM of the EL were 385 nm and 10 nm, respectively. Therefore, we can also fabricate high-power violet LEDs using III-V nitride materials. This InGaN/AlGaIn DH violet LEDs will be very useful for the realization of violet LDs in the near future because the emission is very sharp and strong.

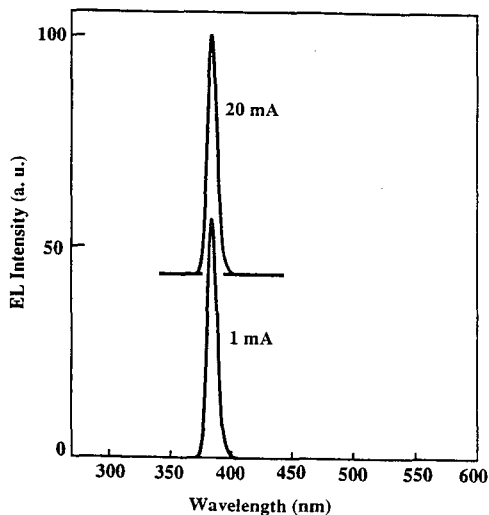


Figure 6. EL spectra of the InGaN/AlGaIn DH violet LEDs under different forward currents.

Figure 7 shows the external quantum efficiencies as a function of the peak wavelength of various commercially available LEDs. Judging from this figure, there are no LED materials except for III-V nitride that have high efficiencies over 1 % below the peak wavelength of 550 nm. Therefore, III-V nitride is one of the most promising materials for LEDs and LDs of peak wavelengths between 550 nm and 360 nm.

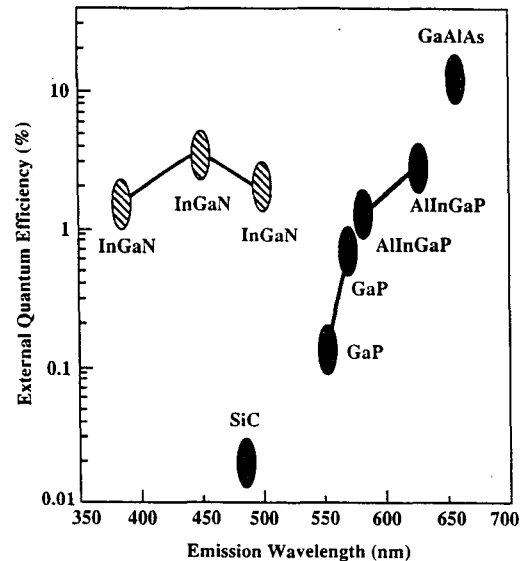


Figure 7. The external quantum efficiencies as a function of the peak wavelength of various commercially available LEDs.

Summary

Highly efficient InGaN/AlGaIn DH blue LEDs with an external quantum efficiency of 5.4 % were fabricated by codoping Zn and Si into the InGaN active layer. The output power was as high as 3 mW at a forward current of 20 mA. The peak wavelength and the FWHM of the EL of blue LEDs were 450 nm and 70 nm, respectively. Blue-green LEDs with a brightness of 2 cd were fabricated by increasing the indium mole fraction of the InGaN active layer. High-brightness blue LEDs with a luminous intensity over 1 cd will pave the way forward realization of full-color LED displays, especially for outdoor use. Also, traffic lights may prove to be a great application for the blue-green LEDs. Total power consumption by traffic lights reaches the gigawatt range in Japan. InGaN/AlGaIn blue-green LED traffic lights, with an electrical power consumption 12% that of present incandescent bulb-traffic lights, promise to save vast amounts of energy. With its extremely long lifetime of several tens of thousands of hours, the replacement of burned-out traffic light bulbs will be dramatically reduced. Using these high-brightness blue-green LEDs, safe and energy-efficient roadway and railway signals will be achieved in the near future.

On II-VI materials, ZnSe/ZnTeSe DH green LED has been reported [21]. The output power, the external quantum efficiency and the peak wavelength of those II-VI LEDs are 1.3 mW, 3.2 % and 512 nm at a forward current of 10 mA. However, a life time of these II-VI LEDs is only a few hundred of hours under room-temperature operation. Because of this poor reliability of II-VI LEDs, LEDs and LDs have never been commercialized. On the other hand, a life time of above-mentioned III-V nitride LEDs is more than a several tens of thousands of hours. The blue and blue-green III-V nitride LEDs are already commercially available with a high reliability. With this high reliability, III-V nitride blue, violet or uv LDs will be realized in the near future.

References

1. W. Xie, D. C. Grillo, R. L. Gunshor, M. Kobayashi, H. Jeon, J. Ding, A. V. Nurmikko, G. C. Hua, and N. Otsuka, "Room temperature blue light emitting p-n diodes from Zn(S,Se)-based multiple quantum well structures," *Appl. Phys. Lett.* **60**, 1999-2001 (1992).
2. K. Koga and T. Yamaguchi, "Single crystals of SiC and their application to blue LEDs," *Prog. Crystal Growth and Charact.* **23**, 127-151 (1991).
3. J. I. Pankove, E. A. Miller and J. E. Berkeyheiser, "GaN electroluminescent diodes," *RCA Review* **32**, 383-392 (1971).
4. S. Nakamura, "Nichia's 1 cd blue LED paves way for full-color display," *Nikkei Electronics Asia*, No. 6, 65-69 (1994).
5. S. Nakamura, T. Mukai, and M. Senoh, "Candela-class high-brightness InGaN/AlGaIn double-heterostructure blue-light-emitting diodes," *Appl. Phys. Lett.* **64**, 1687-1689 (1994).
6. H. Amano, M. Kito, K. Hiramatsu and I. Akasaki, "P-type conduction in Mg-doped GaN treated with low-energy electron beam irradiation (LEEBI)," *Jpn. J. Appl. Phys.* **28**, L2112-L2114 (1989).
7. T. Matsuoka, "Current status of GaN and related compounds as wide-gap semiconductors," *J. Cryst. Growth* **124**, 433-438 (1992).
8. S. Nakamura and T. Mukai, "High-quality InGaIn films grown on GaN films," *Jpn. J. Appl. Phys.* **31**, L1457-L1459 (1992).
9. B. Goldenberg, J. D. Zook and R. J. Ulmer, "Ultraviolet and violet light-emitting GaN diodes grown by low-pressure metalorganic chemical vapor deposition," *Appl. Phys. Lett.* **62**, 381-383 (1993).
10. M. A. Khan, J. N. Kuznia, D. T. Olson, M. Blasingame and A. R. Bhattarai, "Schottky barrier photodetector based on Mg-doped p-type GaN films," *Appl. Phys. Lett.* **63**, 2455-2456 (1993).
11. C. Wang and R. F. Davis, "Deposition of highly resistive, undoped, and p-type, magnesium-doped gallium nitride films by modified gas source molecular beam epitaxy," *Appl. Phys. Lett.* **63**, 990-992 (1993).
12. H. Morkoç, S. Strite, G. B. Gao, M. E. Lin, B. Sverdlov, and M. Burns, "Large-band-gap SiC, III-V nitride, and II-VI ZnSe-based semiconductor device technologies," *J. Appl. Phys.* **76**, 1363-1398 (1994).
13. S. Nakamura, N. Iwasa, M. Senoh and T. Mukai, "Hole compensation mechanism of p-type GaN films," *Jpn. J. Appl. Phys.* **31**, 1258-1266 (1992).
14. J. A. Van Vechten, J. D. Zook, R. D. Horning and B. Goldenberg, "Defeating compensation in wide gap semiconductors by growing in H that is removed by low temperature de-ionizing radiation," *Jpn. J. Appl. Phys.* **31**, 3662-3663 (1992).
15. M. Rubin, N. Newman, J. S. Chan, T. C. Fu and J. T. Ross, "p-type gallium nitride by reactive ion-beam molecular beam epitaxy with ion implantation, diffusion, or coevaporation of Mg," *Appl. Phys. Lett.* **64**, 64-66 (1994).
16. M. S. Brandt, N. M. Johnson, R. J. Molnar, R. Singh and T. D. Moustakas, "Hydrogenation of p-type gallium nitride," *Appl. Phys. Lett.* **64**, 2264-2266 (1994).
17. J. M. Zavada, R. G. Wilson, C. R. Abernathy and S. J. Pearton, "Hydrogenation of GaN, AlN, and InN," *Appl. Phys. Lett.* **64**, 2724-2726 (1994).
18. S. Nakamura, "In situ monitoring of GaN growth using interference effects," *Jpn. J. Appl. Phys.* **30**, 1620-1627 (1991).
19. S. Nakamura, Y. Harada and M. Senoh, "Novel metalorganic chemical vapor deposition system for GaN growth," *Appl. Phys. Lett.* **58**, 2021-2023 (1991).
20. K. Osamura, S. Naka, and Y. Murakami, "Preparation and optical properties of Ga_{1-x}In_xN thin films," *J. Appl. Phys.* **46**, 3432-3437 (1975).
21. D. Eason, J. Ren, Z. Yu, C. Hughes, N. A. El-Masry, J. W. Cook, Jr. and J. F. Schetzina, "Blue & green light emitting diode structures grown by MBE on ZnSe substrates," in Proceedings Abstracts of the Eighth International Conference on Molecular Beam Epitaxy (B11-4, Osaka, Japan, Aug.29-Sept.2, 1994).